Controlling Aggregate Formation in Conjugated Polymers by Spin-Coating Below the Critical Temperature of the Disorder-Order Transition

Markus Reichenberger[1], Daniel Kroh[1], Giovanni M. M. Matrone[2], Konstantin Schötz[1], Stephan Pröller[3], Oliver Filonik[3], Margret E. Thordardottir[3], Eva M. Herzig[4], Heinz Bässler[5], Natalie Stingelin[2,6] and Anna Köhler[1,5,*]

[1] Experimental Physics II, University of Bayreuth, 95440 Bayreuth, Germany

[2] Department of Materials and Center for Plastic Electronics, Imperial College London, London SW7 2AZ, United Kingdom

[3] Herzig Group, MSE, Technische Universität München, Lichtenbergstr. 4a, 85748 Garching, Germany

[4] Dynamics and Structure Formation, University of Bayreuth, 95440 Bayreuth, Germany

[5] Bayreuth Institute of Macromolecular Research (BIMF), University of Bayreuth, 95440 Bayreuth, Germany

[6] School of Materials Science & Engineering and School of Chemical & Biomolecular Engineering, Georgia Institute of Technology, Atlanta Georgia 30332, USA

[*] Corresponding Author: anna.koehler@uni-bayreuth.de

Abstract

Aggregates – i.e. short-ranged ordered moieties in the solid-state of π-conjugated polymers – play an important role in the photophysics and performance of various optoelectronic devices. We have previously shown that many polymers change from a disordered to a more ordered conformation when cooling a solution below a characteristic critical temperature T_c. Using in situ time-resolved absorption spectroscopy on the prototypical semiconducting polymers P3HT, PFO, PCPDTBT and PCE11 (PffBT4T-2OD), we show that spin-coating at a temperature below T_c can enhance the formation of aggregates with strong intra-chain coupling. An analysis of their time-resolved spectra indicates that the formation of nuclei in the initial stages of film formation for substrates held below T_c seems responsible for this. We observe that the growth rate of the aggregates is thermally activated with an energy of 310 meV, which is much more than that of the solvent viscosity (100 meV). From this we conclude that the rate controlling step is the planarisation of a chain that is associated with its attachment to a nucleation centre. The success of our approach for the rather dynamic deposition method of spin-coating holds promise for other solution-based deposition methods.

Keywords:

Dimer, Excimer, Self-assembly, Phase Transition, Solar cells, Low-bandgap polymers, excitonic coupling, film formation, thin films

Table of Contents Figure

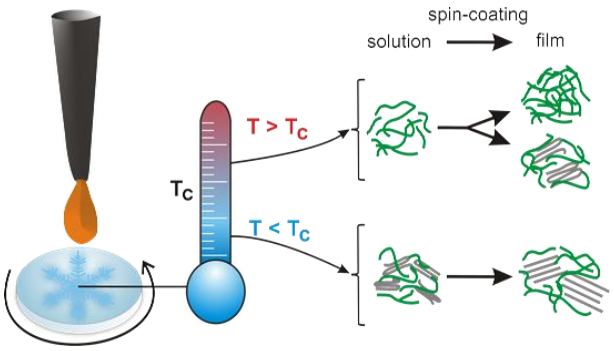

The formation short-range order in thin films during spin-coating can be controlled by chosing a substrate temperature below the critical transition temperature for the disorder-order transition in conjugated polymers. An analysis of time-resolved in-situ absorption spectra indicates that the formation of nuclei for substrates held below T_c is responsible for this. The growth rate of the aggregates is controlled by chain planarisation that is associated with its attachment to a nucleation centre.

1. **Introduction**

In the last few decades, semiconducting conjugated polymers, such as poly(3-hexyl-thiophene-2,5-diyl) (P3HT), have attracted much attention as they combine semiconducting properties with the potential to produce devices via low-cost solution processability.[1-7] A parameter with crucial impact on the performance of organic optoelectronic devices is the solid-state microstructure of the functional layer. Not only long-range order seems important; some degree of short-range molecular order, e.g., resulting from the presence of well-ordered aggregates can have a strong influence on the efficiency of organic solar cells [8-19] and often dictates the performance of organic semiconductors in thin-film field-effect transistors [1, 20-25].

So far, however, only limited approaches have been reported to induce aggregate formation in a controlled fashion, including slow solidification in marginal solvents,[26-29] control of entanglements and sonication,[30-34] and blending[35] – many using poly(3-hexyl thiophene) (P3HT) as model system and many relying on relatively time consuming methodologies. Approaches to control the formation of aggregates during the solution deposition should ideally be based on considering thermodynamics of the solution as well as by taking the kinetics of film formation into account.[9] In particular with respect to the latter, several methods have been reported, such as varying the boiling point of the solvent,[9, 21, 36] varying the deposition time,[37] or adding small amounts of high boiling point solvents such as diiodooctane.[23, 38-44]

Here, we present a versatile and very facile approach that allows to manipulate the formation of such aggregates during solution deposition that can complement and be combined with existing methods. We exploit the fact that many π-

conjugated polymers undergo a disorder-order transition in solution upon cooling,[45-47] and demonstrate that when spin-coating a solution at a temperature below the critical temperature, aggregates already developed in solution dictate formation of important short-range ordered features in the solid state. Beneficially, in many cases, the critical temperature T_c for this transition is near room temperature and, thus, a solution can readily be brought to a temperature above or below T_c as desired. This observation can, though, also explain the large variations in device performance often obtained when processing organic semiconductors as small differences in casting temperature will affect aggregate formation and, as a consequence, the optoelectronic properties of the resulting thin-film architectures.

We demonstrate the general applicability of our approach on the omni-present P3HT, the more rigid poly(9,9-di-n-octylfluorene) (PFO) as another homopolymer, as well as prototypical donor-acceptor polymers such as poly[(5,6-difluoro-2,1,3-benzothiadiazol-4,7-diyl)-alt-(3,3'''-di(2-octyldodecyl)-2,2';5',2'';5'',2'''-quaterthiophen-5,5'''-diyl)] (PffBT4T-2OD or PCE11) and poly{[4,4-bis(2-ethylhexyl)-cyclopenta-(2,1-b;3,4-b′)dithiophen]-2,6-diyl-alt-(2,1,3-benzo-thiadiazole)-4,7-diyl} (PCPDTBT).[16, 41, 48-53] They may differ in their structure formation from homopolymers,[54] and especially compared to the semi-flexible P3HT.[55] We show that for P3HT, PCE11 and PFO, aggregates formed upon spin-coating below T_c have a longer conjugation length and a higher ratio of 0-0 to the 0-1 vibrational peaks in the absorption spectra than when a deposition temperature above T_c is selected; most strikingly, for PCPDTBT, we find that aggregates can only be induced in the film upon spin-coating below T_c. We used spin-coating to demonstrate how

powerful our strategy is, though, we expect straight-forward adaption of our methodology to other deposition techniques and other material systems.

2. Experimental Methods

2.1 *Materials*

The poly(3-hexyl-thiophene-2,5-diyl) (P3HT) with nominally more than 98 % in a head-to-tail connection was purchased from Rieke Metals. It had a number-average molecular weight of $M_n = 18.8\,kg/mol$ and a weight-average molecular weight of $M_w = 38.4\,kg/mol$, i.e. a dispersity of $Đ = 2.04$. It was used in a solution of chlorobenzene (CB) with a concentration of $c = 10\,\frac{g}{l}$ to make films and to measure temperature dependent photoluminescence (PL) in solution.

Poly[(5,6-difluoro-2,1,3-benzothiadiazol-4,7-diyl)-alt-(3,3'''-di(2-octyldodecyl)-2,2';5',2'';5'',2''';5''',2'''-quaterthiophen-5,5'''-diyl)] (PffBT4T-2OD or PCE11) with $M_n = 55\,kg/mol$ and $Đ = 2.1$ was purchased from Ossila. We used it in an ortho-dichlorobenzene (o-DCB) solution with $c = 5\,\frac{g}{l}$ to spin-coat films. In order to determine the critical temperature for the disorder-order transition by absorption measurements, we used a o-DCB with $c = 0.1\,\frac{g}{l}$.

Poly{[4,4-bis(2-ethylhexyl)-cyclopenta-(2,1-b;3,4-b′)dithiophen]-2,6-diyl-alt-(2,1,3-benzo-thiadiazole)-4,7-diyl} (PCPDTBT) was purchased from 1-Material and had $M_n = 23\,kg/mol$ and $Đ = 1.7$. As for P3HT, we used it in a CB solution with $c = 10\,\frac{g}{l}$.

Poly(9,9-di-n-octylfluorene) (PFO) of $M_n = 31\ kg/mol$ and $Đ = 2.9$ was obtained from American Dye Source and used in 2-methyl-tetrahydrofurane (MTHF) with a concentration $c = 3\ \frac{g}{l}$ for spin-coating films containing β-phase. To spin-coat an amorphous film, we used a toluene solution of $c = 20\ \frac{g}{l}$. The batch of PFO used for this study is the same as in ref. [45].

As solvents for spin-coating, we used CB, which has a boiling point of 132 °C, o-DCB with a boiling point of 180 °C, MTHF (boiling point at 80 °C) and toluene (boiling point at 111 °C). All solvents were anhydrous and obtained from Sigma-Aldrich. They were used in a glovebox after filtering with a filter of 0.2 µm pore size.

2.2 Film preparation and in situ temperature dependent absorption measurements

The solutions were fabricated in a glove-box under nitrogen atmosphere by mixing the anhydrous solvent with the polymer. The solutions were stirred at 40 °C with about 400 rpm for several hours and after this filtered through a 0.2 µm filter. All the polymer solutions were heated to about 60 °C prior to deposition such as to dissolve potential existing aggregates. In a second glovebox with argon atmosphere, the room-temperature solutions were deposited onto substrates held at different substrate temperatures. Spin-coating took place at 400 rpm or, in the case of PFO, at 800 rpm. The substrates were round quartz substrates, with a diameter of 13 mm, lying on top of a temperature controlled sample holder of a home-built spin- coater.[56]

The cooling (heating) of the spin-coater was performed by surrounding the sample holder with a flow of cold nitrogen gas (hot air). The temperature can be adjusted by

controlling the pressure of the gas flow and is measured with a digital Keithley 2000 multimeter connected to a positive temperature coefficient (PTC) thermometer PT 1000, the latter being pressed onto the spectrosil surface, directly before dropping the solution. Any change in substrate temperature during the solvent evaporation process due to the latent heat of evaporation is not considered.

To allow for the absorption measurements, the spin-coater has a white light LED as light source underneath the substrate and a glass fibre for detection of the transmitted light above. This design is similar to that reported by Abdelsamie et al. [57] The fibre is attached to a MS125 spectrograph from Oriel Instruments with a charge-coupled device (CCD) camera from Andor-Solis that takes one picture every 60 ms.

Steady state UV-VIS absorption spectra were taken by using a Cary 5000 UV/VIS spectrometer with an integrating sphere from Varian.

2.3 Optical characterization of solutions

Absorption and photoluminescence spectra taken on solutions at different temperatures were acquired using a home-built setup. It consists of a wolfram lamp as light source for absorption measurements, a 405 nm (3.06 eV) continuous-wave diode laser from Coherent for excitation in emission measurements and a spectrograph Shamrock SR303i with an Andor iDus CCD-camera for detection. The solutions were measured in a 1 mm fused silica cuvette that was placed in a temperature-controlled continuous flow helium cryostat from Oxford Instruments. We waited for 15 min after

reaching a new temperature for the temperature to be fully equilibrated before taking the measurement.

2.4 Characterization of crystal structure in thin films

Grazing incidence wide angle X-ray scattering (GIWAXS) measurements have been carried out at the Sirius beamline (Soleil, France) to characterize the P3HT crystal structure for the different coating temperatures. Experiments were carried out at 8keV with a sample detector distance of 32.5 cm using a Pilatus 1M detector at an incident angle of 0.18°. The 2d data is reduced to 1d cuts in the horizontal direction using the GIXSGUI software.[58]

3. **Results and Discussion**

3.1 Aggregate formation in P3HT

A conjugated polymer, for which the formation of aggregates has been studied extensively and that therefore serves as an excellent model system to start our study, is poly(3-hexyl-thiophene-2,5-diyl) (P3HT) (Figure 1). It shows a well-known disorder-order transition upon cooling in solution, with a critical temperature T_c that depends on the molecular weight and dispersity of the polymer.[45, 59-60] Panzer et al. recently reported a T_c of about -8 °C (265 K) when depositing P3HT in a MTHF solution with a concentration $c = 0.1 \frac{g}{l}$.[59] To obtain good films during spin-coating, we used for the same batch of P3HT as Panzer et al. used a relatively concentrated solution of $c = 10 \frac{g}{l}$ in chlorobenzene (CB).

We found this slightly raises the critical temperature to a value between 5 °C and 0 °C, i.e. $T_c \approx (-2 \pm 2)\,°C$, as evidenced by temperature-dependent photoluminescence measurements presented in Figure S1 in the Supporting Information (SI).

In order to elucidate the process of aggregate formation upon spin-coating, we employed a home-built spin-coater that allowed to in situ monitor the absorption spectra during the spin-coating processes while controlling meticulously the deposition temperatures; we selected two deposition temperatures above T_c (i.e. 22 °C and 10 °C), one near T_c (i.e. 0 °C), and one below T_c (i.e. -5 °C). The solution was kept at room temperature in all cases. Exemplary in situ time-resolved absorption spectra for a deposition temperature of 10 °C are displayed in Figure 1a; Figure S2 in the SI summarizes the data obtained for all four temperatures. The spin-coating time is shown as abscissae, while the photon energy (wavelength) is shown as ordinate below (on top). The optical density (OD) is indicated by the colour from blue ($OD \leq 0.1$) to red ($OD \geq 0.9$). The top panel shows the absorption spectra at 0 s and 100 s, and the right panel shows the time evolution of the absorption at 2.05 eV, where only aggregates absorb, and at 2.75 eV, where only disordered chains absorb.

For all deposition temperatures, we observe the same general behaviour. Initially, we see a broad and unstructured absorption spectrum centred at 2.70 eV (black line in Figure 1a) that is characteristic for non-aggregated chains.[36, 61] Within the first few seconds of the spin-coating process, .a part of the polymer solution is splattered off the sample due to the centrifugal forces induced by spincoating. The reducing amount of solvent on the substrate is reflected in a reducing optical density at 2.75 eV (green line in Figure 1a). The subsequent plateau in the time-evolution of the absorbance suggests that

there is no further loss of material. From 56 s to 75 s, the absorbance at 2.75 eV is getting less pronounced and an absorption feature at 2.05 eV appears, the intensity of which does not change beyond 75 s. These observations illustrate that during spin-coating, the solvent evaporates and thus the polymer concentration in the liquid film increases.[62] At a certain point, a critical concentration is reached where aggregates form spontaneously leading to well-defined features in the absorption spectrum (shown in magenta in Figure 1a/top panel) with vibronic peaks at 2.05 eV, 2.24 eV, and 2.40 eV, indicating that H-type aggregates form.

We can trace the formation of these aggregates in more detail by monitoring the absorption of the 2.05 eV peak as a function of time for all deposition temperatures used. These transformation curves are shown in Figure 1b, with the maximum value of aggregate absorption normalized to unity. While the curves for the samples cast at 22 °C and 10 °C show a clear sigmoidal shape with a sharp onset in the fraction of aggregates, the curves obtained from the films deposited at 0 °C and -5 °C show a long drawn-out "onset" in the fraction of aggregates followed by an accelerated transformation once 50% of the aggregates have formed – a time we refer to as $t_{0.5}$ (see also Figure S3 in the SI). The drawn-out "onsets" for the transformation curves for samples cast at 0 °C and -5 °C suggest that aggregates may already be present in solution prior to the actual transformation that takes place near $t_{0.5}$. These aggregates likely form when the solution adopts the substrate temperature near or below T_c. When defining the transformation rate as $1/t_{0.5}$,[63] we obtain values for the transformation rate of 23 ms^{-1} using a deposition temperature of 22 °C, 15 ms^{-1} for 10 °C, 10 ms^{-1} for 0 °C and 7 ms^{-1} for -5 °C. When plotting the thus-obtained transformation rates against inverse temperature on a semi-

logarithmic scale (see Figure 1c), a linear slope results that indicates a thermally activated behaviour with an activation energy of about 310 meV, i.e. about ten times the thermal energy at room temperature. Further data and a time-temperature-transformation (TTT) curve [63] are given in Table S1 and Figure S3 of the SI. The increase of the transformation rate with temperature indicates that the formation of the aggregates is not limited by nucleation. This is also evident by the observation that the presence of aggregates, i.e. possible nucleation sites, in the solution on the 0 °C and -5 °C substrates does not accelerate the overall rate of aggregate formation.

The fact that our rates actually fit to a thermally activated process suggests that the formation process of the aggregates is controlled by the product of the probabilities that a chain segment may diffuse towards an already existing nucleation centre and that it may attach to it, i.e. “react”. If both processes – i.e. diffusion and “reaction” – are thermally activated, then the net activation energy is the sum of both energies. In the current case, the diffusion of the chain segments can be assumed to be controlled by the inverse of the solvent viscosity, and the associated activation energy for CB is 100 meV.[64] Since the measured activation energy for the growth of the aggregates is 310 meV, it appears that adding a chain to a nucleation centre or pre-existing aggregate requires an activation energy of roughly 200 meV. When inducing aggregate formation in P3HT or other polymers by cooling a solution, we have observed that an increase in the effective conjugation length, attributed to a planarization of the chain backbone, occurs immediately prior to the actual phase transition[45, 65] (NB.: this process cannot be resolved in the case of aggregate formation during soldification[44]). We thus conclude that aggregation is associated with an increase in planarization of a chain segment and attribute the additional required activation energy of 210 meV with the planarization of the chain segment before

its attachment to a nucleation centre. This is consistent with calculations by De Leener et al. made to describe the aggregation of MEH-PPV.[66]

Clearly other aspects could lead to our observations. In order to confirm that the appearance of aggregates in films cast at 0 °C and -5 °C is due to the liquid film adopting the substrate temperature around T_c, rather than due to the increased time needed for transformation, we also spun films at 22 °C from a $c = 10\,\frac{g}{l}$ solution with o-DCB. This solvent has a boiling point of 180 °C compared to CB which has a boiling temperature of 132 °C. The higher boiling point of this solvent and, thus, the slower solidification of the systems, shifts the onset time for transformation so that it nearly coincides with that the sample spun at -5 °C from CB, as shown in Figure 1b; yet, in contrast to the latter sample, there are no aggregates formed prior to the transformation. This illustrates that the use of a deposition temperature below T_c is causing the presence of aggregates prior to the transformation, as expected.

To assess the impact on the final solid-state structures of initial aggregates formation in solution via casting at temperatures below T_c, we analyzed the absorption spectra as shown exemplarily in Figure 1d for samples cast at 10 °C. Following the approach outlined previously, we separate the final film spectra into the contributions from disordered chains and from aggregated chains.[36, 44, 61] For this, we normalize the absorption spectrum of the disordered chains – obtained at the very beginning of the spin-coating process – such as to match the high energy tail of the film spectrum. The difference between film spectrum and the disordered chain spectrum is assigned to the absorption from the aggregates. The *fraction of absorption* from aggregated chains for P3HT films spin-cast at 22 °C, 10 °C, 0 °C and -5 °C is 52%, 50%, 51% and 45%

respectively (see Figure S4 in the SI for all four temperatures). The *fraction of aggregated chains* can be calculated from the *fraction of absorption* by considering that, for P3HT, the oscillator strength of aggregated chains is about 1.4 times higher than the one of nonaggregated chains.[36, 45, 61] We confirmed that this is still the case when spin-coating samples using different deposition temperatures. The fraction of aggregated chains stays about the same (36 ± 1%) in films spin-cast at 22 °C, 10 °C and 0 °C, and slightly decreases to 32% in the film cast at -5 °C. Moreover, the amount of aggregates remains essentially unaltered when spin-coating from o-DCB at 22 °C instead of CB (Figure S5a in the SI) – all demonstrating that the amount of aggregates formed in the final polymer film remains essentially unaltered by the spin-coating temperature and condition.

While the presence of aggregates prior to solidification does not accelerate the transformation nor increase the amount of aggregates formed, it is important to note that is alters *the character* of the aggregates in the film. Figure 1e compares the absorption from the aggregates obtained from casting a P3HT solution from CB using different deposition temperatures. It is evident that the aggregates in films cast at 0 °C and -5 °C films have a higher 0-0 peak than those deposited at 22 °C and 10 °C films, or the film spin-cast from o-DCB (see Figure S5b in the SI), in agreement with the blend work by Hellman et al.[67] The ratio between the 0-0 and the 0-1 peaks in absorption can be taken as a measure for the coupling strength in weakly interacting H-aggregates according to models suggested by Spano and coworkers.[61, 68-70] If we apply the associated analysis to the spectra as detailed in ref. [71] (see Figure S6 in the SI for full details), we find that the free exciton bandwidth W of the aggregates in the P3HT films decreases with reducing

deposition temperature, from 70 meV to 27 meV in the temperature range between 22 °C and -5 °C (Figure 1f). These values are typical for P3HT.[61]

The difference in the character of the aggregates is even more visible during the formation process. Figure 2 shows the absorption spectra taken at different times during the transition, comparing the spin-coating process using different deposition temperatures. The spectrum at time $t_{0.5}$, where half of the total amount of the aggregates has formed, is shown as blue solid line for each temperature. For the two sample spun using deposition temperatures $T > T_c$, we observe an isosbestic point at 2.60 eV that results from the transformation of disordered chains into chains with weak H-type interaction.[36, 44, 59, 61] The 0-0 peak in absorption for these two samples is centred at about 2.05 eV (Figures 2a and 2b). In contrast, for the samples cast at $T \leq T_c$ (Figures 2c and 2d), there seems to be an "isosbestic" point at 2.45 eV for times shorter than $t_{0.5}$, followed by an abrupt change to a second "isosbestic" point at 2.64 eV for times larger than $t_{0.5}$. Further, the spectra taken in the first half of the transformation process show a well-resolved 0-0 peak centred at 2.00 eV, suggesting a longer conjugation length, that moves to higher energies and loses structure in the second half of the transformation. From this we conclude that, as a result of the cold substrate temperature, H-type aggregates form in the still liquid film that are characterized by a longer conjugation length and concomitantly weaker electronic interaction between the polymer chains. When the solvent finally fully evaporates in the second half of the transformation process, the intra-chain order of these chains gets disturbed which slightly reduces the conjugation length of the aggregates already formed. Nevertheless, as evidenced in Figure 1e, overall

the aggregates formed upon spin-coating onto the cold substrates still have a higher 0-0 peak, testifying to a lower exciton bandwidth yet longer conjugation length.[36]

This result can be supported by GIWAXS measurements on the final P3HT thin films after deposition at the four temperatures. The signal responsible for the π-stacking distance shows two length scales for all temperatures (see Figure S7 in the SI). While the samples for 10 °C and 22 °C show a balanced ratio or simply a broad range of separations, the π-stacking distance clearly increases for the lower deposition temperatures, consistent with the reduction of electronic interaction.

This change in the character of the resulting aggregates is akin to that obtained when adding a small amount of a high boiling point additive, such as 1,8-diiodooctane (DIO) to the solution. Upon adding 3 wt% DIO to a CB solution of P3HT, the exciton coupling strength reduces by about a factor of two, similar to the effect seen here upon spin-coating onto a substrate with $T \leq T_c$. However, the additive DIO has been shown to remain in film for hours and days, causing an ongoing crystallization and thus morphological changes over days. Such ongoing crystallization does not occur when spin-coating onto a substrate with $T \leq T_c$. Spectra of fresh films and films after one day show no change (see Figure S8 in the SI). This likely will be beneficial for device fabrication as it may turn out to assist long-term stability. More broadly, the above shows that we were able to control formation of aggregates of a lower free exciton bandwidth, and concomitantly longer conjugation length, simply by appropriate choice of deposition temperature for spin-coating. For this, we do not require any pre-processing of the casting solution such as using solvent additives or solvent mixtures or post-processing of the spin-cast film, e.g. by thermal or vapor annealing, and the resulting films are morphologically

stable. This is therefore seems to be a suitable approach to be explored further for application to other, more industrially relevant solution processing methods such as slot-die coating or ink-jet printing. However, before advancing in such a direction, it is worthwhile to consider whether our result applies merely to P3HT or whether it is more generally applicable to other semiconducting polymers. For this, we considered PFO and two polymers frequently used in organic solar cells that have transition temperatures near room temperature, that is PCE11 and PCPDTBT.[16, 48-52]

3.2 Aggregate formation of PCE11

PCE11, also known as PffBT4T-2OD, is attracting much interest in the field of organic semiconductors, as it enables high mobility and solar cell devices with up to 10.8% efficiency.[16] In order to determine the critical temperature for the disorder-order transition in solution, we measured the absorption of PCE11 in an o-DCB solution with a concentration $c = 0.1\,\frac{g}{l}$ as a function of temperature (Figure 3a). The disorder-order transformation in PCE11 follows the pattern recently reported for other polymers.[45] Upon cooling from 400 K until 320 K, the absorption band, centered at 2.30 eV at 400 K, shifts by about 100 meV to the red spectral range, indicating an increase in conjugation length or backbone planarization. From 320 K onward, a structured lower energy absorption band emerges with vibrational peaks at 1.78 eV and 1.97 eV at 240 K. Due to the similarity in spectral behaviour to the disorder-order transformation in other conjugated polymers, we attribute this band to the formation of aggregates of PCE11. The critical temperature for the phase transition is therefore about 320 K, i.e. about 47 °C. In order to spin-coat films, a higher concentration of $c = 5\,\frac{g}{l}$ is required. From comparison to P3HT it is

reasonable to presume that T_c will change only moderately with temperature. Hence, for spin-coating we choose 70 °C as a substrate temperature above T_c and 22 °C as deposition temperature below T_c.

Similar to the study with P3HT, the kinetics of film formation during spin-coating of PCE11 from an o-DCB solution at the different substrate temperatures above and below below T_c is monitored by in situ time-resolved absorption spectra, which are depicted in Figure 3b for 70 °C and in Figure 3c for 22 °C (more detail in Figure S10 in the SI).

When spin-coating PCE11 in o-DCB onto a substrate held at 70 °C, i.e. above T_c, the absorption spectra taken at different times during spin-coating can be grouped into three time ranges, as depicted in Figure 3d. The spectra in the top panel, where material loss still takes place (first time range), are normalized to their absorbance at 2.25 eV whereas the spectra in the middle (second time range) and bottom panel (third time range) are merely corrected for the baseline. In the first time range, which is from 0 s to 3.9 s, we observe a broad and unstructured absorption spectrum centred at 2.25 eV. We attribute this absorption to disordered chains of PCE11. In the second time range, from 4.0 s to 5.0 s, this absorption reduces in intensity and a lower energy band appears with a 0-0 peak at about 1.8 eV. The spectra show an isosbestic point at 2.15 eV. In the third time range, which is between 5.0 s and about 60 s, no further changes are observed. Based on earlier work, we associate the resulting thin film spectrum with a superposition of absorption from remaining disordered chains and aggregated chains.[36, 44, 72] Evidently, there seems to be a critical concentration that facilitates aggregate formation as the solvent evaporates, consistent with calculations made for the poly(p-phenylene deriatrive) MEH-PPV.[66]

A rather different process is observed when spin-coating a PCE11 solution in o-DCB at 22 °C, i.e. below T_c (Figure 3e). Then the absorption spectra taken at different times during spin-coating do not show any differences in spectral shape. Rather, the structured band with a 0-0 peak at about 1.8 eV, superimposed by the broad band centred at 2.3 eV, appears right from the beginning of the spin-coating process. Considering that there is a maximum fraction of ordered domains that can be realized in a film taking into account entropic reasons, the observation that the fraction of aggregates stays the same upon spin-coating, i.e. in the solution and in the film, suggests that this maximum fraction is already realized in solution and film. We recall that for PCPDTBT, Scharsich et al also observed the same maximum fraction of aggregates in both, solution and film.[73] We point out that in PCE11, the solution, kept at room temperature prior to the spin-coating process, is at a temperature below T_c ($T_c \approx 47$ °C) so that aggregates will already be present. This is slightly different from P3HT, where the room temperature solution is above T_c ($T_c \approx$ -2 °C) so that initial aggregates only form in the liquid film within the first few seconds as the liquid film adopts the substrate temperature near or below T_c.

Figure 3f compares the absorption from the aggregates formed in PCE11 by spin-coating above and below T_c, normalized to their 0-1 peak at 1.94 eV. In order to obtain only the aggregate absorption, the spectra of the spin-cast films have been separated into the contributions from the disordered chains and the aggregated chains in the same way as presented above for P3HT, and as detailed in Figure S10 in the SI. The fraction of absorption from aggregated chains for PCE11 films spin-cast at 70 °C and 22 °C are 64% and 67%, respectively, i.e., rather similar for the two sample. We observe that the aggregate absorption of the film spun at 22 °C is located at slightly lower energies and

has a higher 0-0/0-1 peak ratio compared to the aggregate absorption spectrum at 70 °C. This is analogous to P3HT and indicates a stronger delocalization along the polymer chain with concomitantly reduced inter-chain coupling.[61, 68, 70, 74] Thus for both P3HT and PCE11, we find that spin-coating onto a substrate below T_c does not significantly impact on the amount of aggregates formed, yet it does change the character of the resulting aggregates such that the electronic coupling along the chain is increased whereas the coupling between chains reduces. Sometimes, this is referred to as increasing the J-type compared to the H-type characteristics.[70, 74] It is noteworthy that we found this trend for both aggregates, those of P3HT that are of a predominant H-type character as well as for those of PCE11, which are characterized by a peak ratio of the 0-0/0-1 absorption peaks exceeding one, that can indicate a disordered mixed HJ-like nature.[74]

3.3 Extension to PCPDTBT and PFO

We extend our studies to the low-bandgap copolymer PCPDTBT and to the higher bandgap homopolymer PFO to illustrate the broader applicability of our approach, as well as to draw attention to the subtle variations that may occur from polymer to polymer. PCPDTBT and its derivatives are widely used in efficient organic solar cells.[48-52] In part, the good performance of these cells is a result of the high degree of (short-range) order that can be obtained in blends with PCBM. Scharsich et al. have demonstrated that PCPDTBT has its T_c around 27 °C for a MTHF solution with a concentration $c = 0.25 \frac{g}{l}$.[73] They used the same batch of polymer for their studies than we use here. Based on the results obtained with P3HT, we estimate that a similar T_c applies for a CB solution with

$c = 10\,\frac{g}{l}$. Hence, for spin-coating we choose 60 °C as substrate temperature above T_c and 22 °C as deposition temperature below T_c.

When spin-coating a PCPDTBT solution in CB at 60 °C, i.e. above T_c, the absorption spectra taken at different times during spin-coating (Figure 4a) are broad, unstructured and centered around 1.78 eV, characteristic for disordered polymer chains. Moreover, they do not change shape during spin-coating, so that the normalized spectra of the initially liquid, just deposited film and of the final, dry film coincide. Comparison with Scharsich et al. shows that these spectra indicate an amorphous film with solely disordered chains. In contrast, when spin-coating a PCPDTBT solution in CB at 22 °C, i.e. below T_c, the absorption spectra taken at different times during spin-coating change such that a lower energy shoulder appears from about 20 s after deposition onward (Figure 4b). The difference between the initial and final spectrum is shown as green line in Figure 4b, with a peak apparently centered at 1.6 eV. This apparent peak position is due to the fact that the sensitivity range of the detector ends at about 1.5 eV (approximately 830 nm). Comparison with the data by Scharsich et al. [73], shown for ease of reference in Figure 4c, indicates that the additional contribution in the red spectral range can be attributed to aggregated chains with a disordered mixed HJ-like character. Thus, the fact that for PCPDTBT T_c is above room temperature assists the formation of aggregates even for a highly disordered deposition method such as spin-coating, since aggregation is thermodynamically favored below T_c.

In a similar way, the character of the β-phase aggregates in PFO changes as indicated by an increase in the ratio of the 0-0 to the 0-1 peak when lowering the substrate temperature. PFO has a T_c of 245±15 K (-27±15 °C) for a solution of MTHF at a

concentration of $c = 0.25\,\frac{g}{l}$.[45] The broad distribution results from the polydispersity of the sample, with longer chains having a higher T_c.[59] Thus, the longest chains in a dilute solution begin to aggregate near -10 °C. As the absorption range of PFO exceeds the spectral range of our time-resolved setup, steady-state spectra were taken of the spin-cast films using a commercial UV-Vis spectrometer. Figure 4d shows the absorption spectra of PFO films spun from MTHF solution, with a concentration of $c = 3\,\frac{g}{l}$, onto substrates held at 22 °C, -10 °C and -20 °C. The increase in the height of the peak at 2.86 eV is well evident. This peak is characteristic for the β-phase.[41, 46, 53] In order to assess whether this merely indicates a change in the amount of β-phase formed or whether this is also associated with a change in the character of the aggregates, we have separated the spectra into the contributions from the β-phase and from the disordered phase. For this, we measured an absorption spectrum for an amorphous film, obtained by spin-coating from toluene, normalized it to fit the high energy tail of the absorption bands in Figure 4d and subtracted it, as detailed in Figure S11 in the SI. The resulting aggregate spectra are normalized to the 0-1 peak and shown in Figure 4e. Upon spin-coating, near or below T_c, the relative intensity of the 0-0 peak increases while that of the 0-2 peak at 2.25 eV decreases. While the overall character still resembles a weakly interacting H-aggregate, lowering the substrate temperature clearly increases the coupling along the chain.[61, 68, 70, 74]

4. Conclusion

While polymer conformation and associated film morphology are often difficult to adjust in a systematic manner, they can be a decisive factor for the performance of organic

semiconductor devices. In previous studies we have shown that many polymers undergo a coil-globule-like transition when cooling a solution below a certain critical temperature T_c.[45] This transition can be modelled by common theoretical approaches that, for example, predict an increase in T_c with molecular weight, or an increasing abruptness of the transition with high chain rigidity or lower polydispersity. [75-76] We demonstrate here that the critical temperature can be employed as a parameter in the solution-deposition process to control which type of aggregates form. This applies even to a rather dynamic deposition method such as spin-coating with a fast rotating substrate. Moreover, the rate of aggregate growth during the solidification process is thermally activated, with about 100 meV of the activation energy being associated with the solvent viscosity, yet a further 210 meV being required to increase the planarization of the chain segment.

Using P3HT and PCE11 as main examples, we have shown that choosing a substrate temperature near or below T_c results in aggregates with a higher ratio of the 0-0/0-1 absorption peak than when a substrate above T_c is used. Based on Spano et al., we interpret the higher peak ratio to indicate more electronic coupling along the chain and less inter-chain coupling.[61, 68, 70] Regarding the mechanism for this phenomenon, we consider that for substrates held at or below T_c, aggregates will form as soon as the deposited solution has adopted a temperature close to T_c within the first couple of seconds. At this stage, there is still some solvent present in the film that can facilitate the formation of planarized chromophores with good intra-chain coupling. We speculate that these may serve as nuclei during the eventual transformation process. As there may be some vertical temperature gradient across the film, the density of nuclei may vary accordingly. In contrast, when spin-coating on substrates above T_c, preformed aggregates

may not be available in a similar manner. Our results are further corroborated and differentiated for the polymers PCPDTBT and PFO.

These initial exploratory insights hold significant potential for further developments. Transition temperatures near room temperature are not uncommon for today's efficient low-bandgap polymers, so that our approach may easily be adapted to more compounds. Furthermore, it implies that future synthetic work may need to consider tailoring T_c for specific applications, e.g. by modifying molecular weight, polydispersity or torsional rigidity. Finally, it will be interesting to explore to which extent our result may be transferrable to more steady deposition approaches such as the technologically relevant slot-die coating, or to the deposition of blends.

MR, DK, GMMM and KS took all absorption spectra. MR analysed the spectra under the direction of AK, NS and HB. SP, OP and MET have carried out the GIWAXS measurements, EMH carried out the corresponding analysis. MR, NS, HB and AK discussed the results and wrote the manuscript.

Acknowledgements

We gratefully acknowledge support from the Hanns-Seidel-Stiftung through a stipend to MR by funds from the German Federal Ministry of Education and Research (BMBF), support from the German Science Foundation (DFG) through the Research Training Group GRK 1640 "Photophysics of Synthetic and Biological Multichromophoric Systems" and from the State of Bavaria through the Research Network "Solar

Technologies go Hybrid” as well as the “Energy Valley Bavaria”. We thank Ioan Botiz and Peter Strohriegl for fruitful discussions. Finally, we gratefully acknowledge support via the Marie Skłodowska-Curie Actions Innovative Training Networks ‘H2020-MSCA-ITN-2014 INFORM –675867’ that provided a unique platform for scientific discussions and student exchanges.

Supporting Information

The supporting information contains: Temperature-dependent PL of P3HT (S1); In situ time-resolved absorption during spin-coating from a P3HT solution in CB at different substrate temperatures (S2); A table detailing the kinetics of P3HT aggregation (T1) and associated figures (S3); Absorption of P3HT films spun onto substrates held at different temperatures and associated analysis (S4); Comparison to P3HT spun from o-DCB solution (S5); Franck-Condon progressions of P3HT aggregates for all substrate temperatures (S6); GIWAXS 2d data and horizontal cuts for the films spun with different deposition temperatures (S7); Absorption of P3HT films taken fresh and after one day (S8); In situ time-resolved absorption spectra during spin-coating from a PCE11 solution in o-DCB at different substrate temperatures (S9); Absorption of a PCE11 spun onto substrates at 70 °C and 22 °C and associated analysis (S10); Absorption of a PFO spun onto substrates at 22 °C, -10 °C and -20 °C and associated analysis (S11).

Figures and Figure Captions

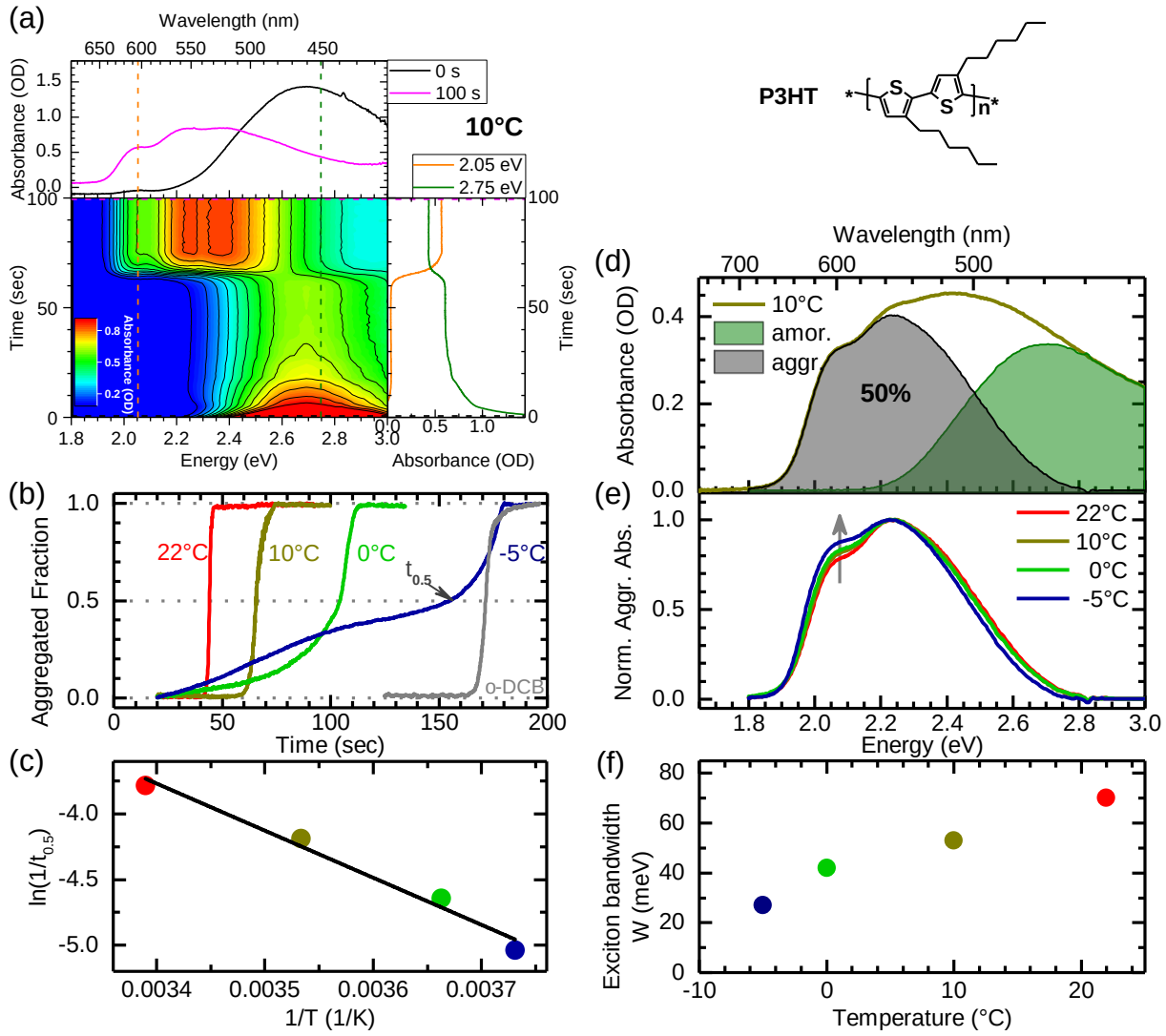

Figure 1: Spin-coating a solution of P3HT in CB ($c = 10\ \frac{g}{l}$) at different substrate temperatures, i.e. 22°C, 10°C, 0°C and -5°C, and in o-DCB (grey line) at 22°C. The chemical structure of P3HT is shown on the top right. (a) In situ time-resolved absorption spectra during spin-coating, exemplarily for 10°C. (b) Transformation curves obtained by monitoring the absorption at 2.05 eV for the four different substrate temperatures. The centred dotted line helps to identify the times $t_{0.5}$ until 50% of the transformation has completed. (c) The transformation rate against inverse temperature on a semi-logarithmic scale. (d) Absorption spectrum of a P3HT film after spin-coating

taken in an integrating sphere (thick coloured line), exemplarily for 10°C. The spectrum is separated into contributions attributed to aggregated polymer chains (black filled line) and nonaggregated polymer chains (green filled line). The number denotes the value for the fraction of absorption from aggregated chains. (e) Aggregate absorption spectra of P3HT films after spin-coating at different temperatures, normalized to their maximum. The grey arrow is a guide to the eye. (f) Free exciton bandwidth W of the aggregates in P3HT films as a function of substrate temperature.

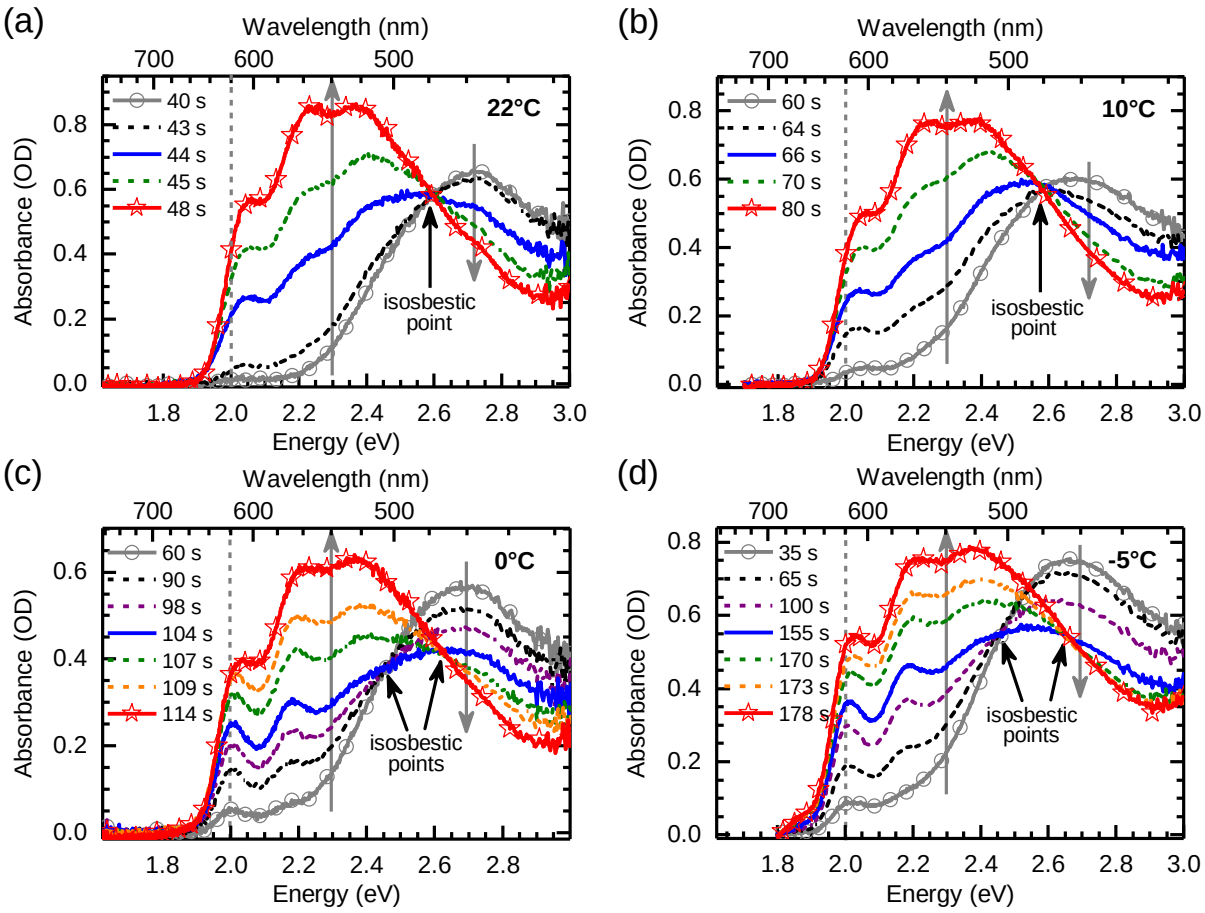

Figure 2: Absorption spectra taken at different times in the transition range during spin-coating of a P3HT solution in CB at different substrate temperatures, i.e. (a) 22°C, (b) 10°C, (c) 0°C and (d) -5°C. The spectrum at time $t_{0.5}$, where half of the total amount of the aggregates has formed, is shown as blue solid line for each temperature. The spectra are set to zero at 1.8 eV to account for the offset due to scattering. The grey dashed lines are a guide to the eye, as well as the grey arrows, which indicate the evolution of the spectra with increasing time.

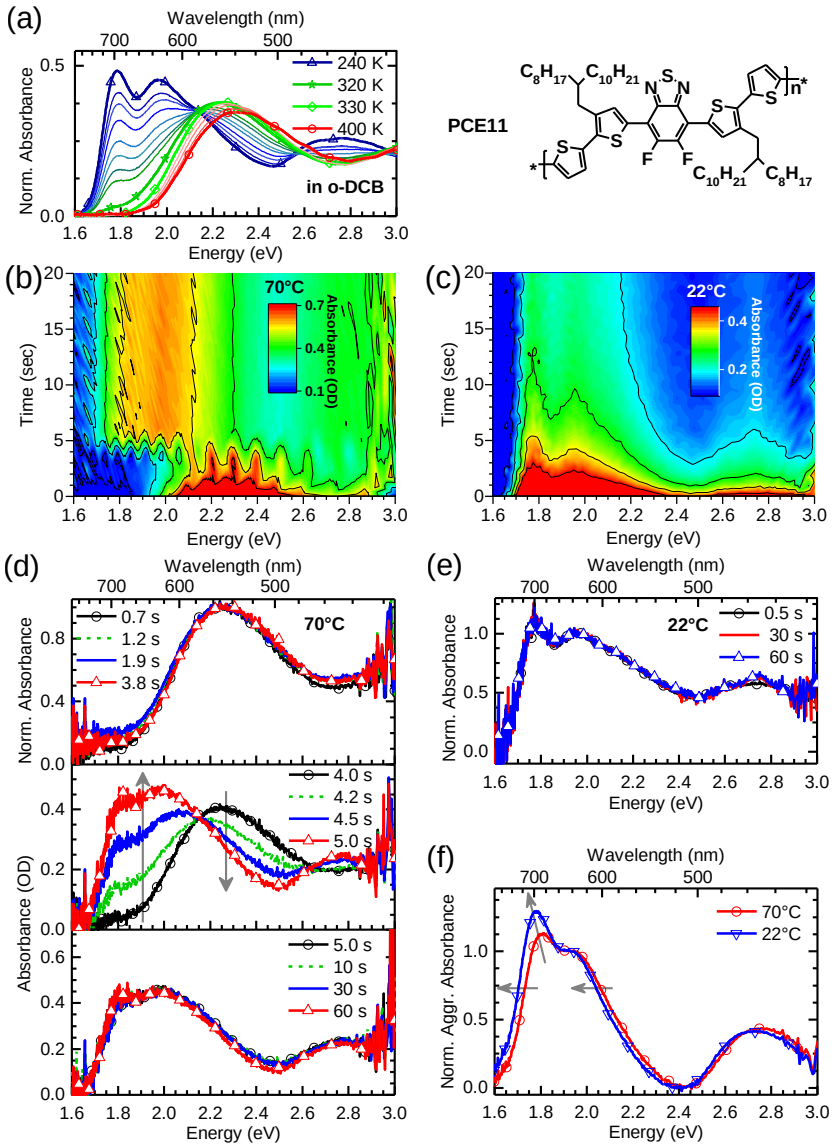

Figure 3: (a) Absorption spectra of a PCE11 solution in o-DCB ($c = 0.1\,\frac{g}{l}$), taken at different temperatures upon cooling the solution. The chemical structure of PCE11 is shown on the top right. (b,c) In situ time-resolved absorption spectra during spin-coating of a PCE11 solution in o-DCB ($c = 5\,\frac{g}{l}$) at different substrate temperatures, i.e. 70°C and 22°C. (d) Absorption spectra taken at different times during spin-coating onto a substrate at 70°C. The spectra are grouped into three time ranges, as described in the text. The spectra are normalized at 2.25 eV in the top panel and they are baseline corrected in the middle and bottom panel. (e) Absorption spectra taken at different times during spin-coating onto a substrate at 22°C, normalized at 1.94 eV. (f) Aggregate

absorption spectra taken of a PCE11 film after spin-coating at 70°C and at 22°C, normalized at 1.94 eV. The grey arrows are a guide to the eye.

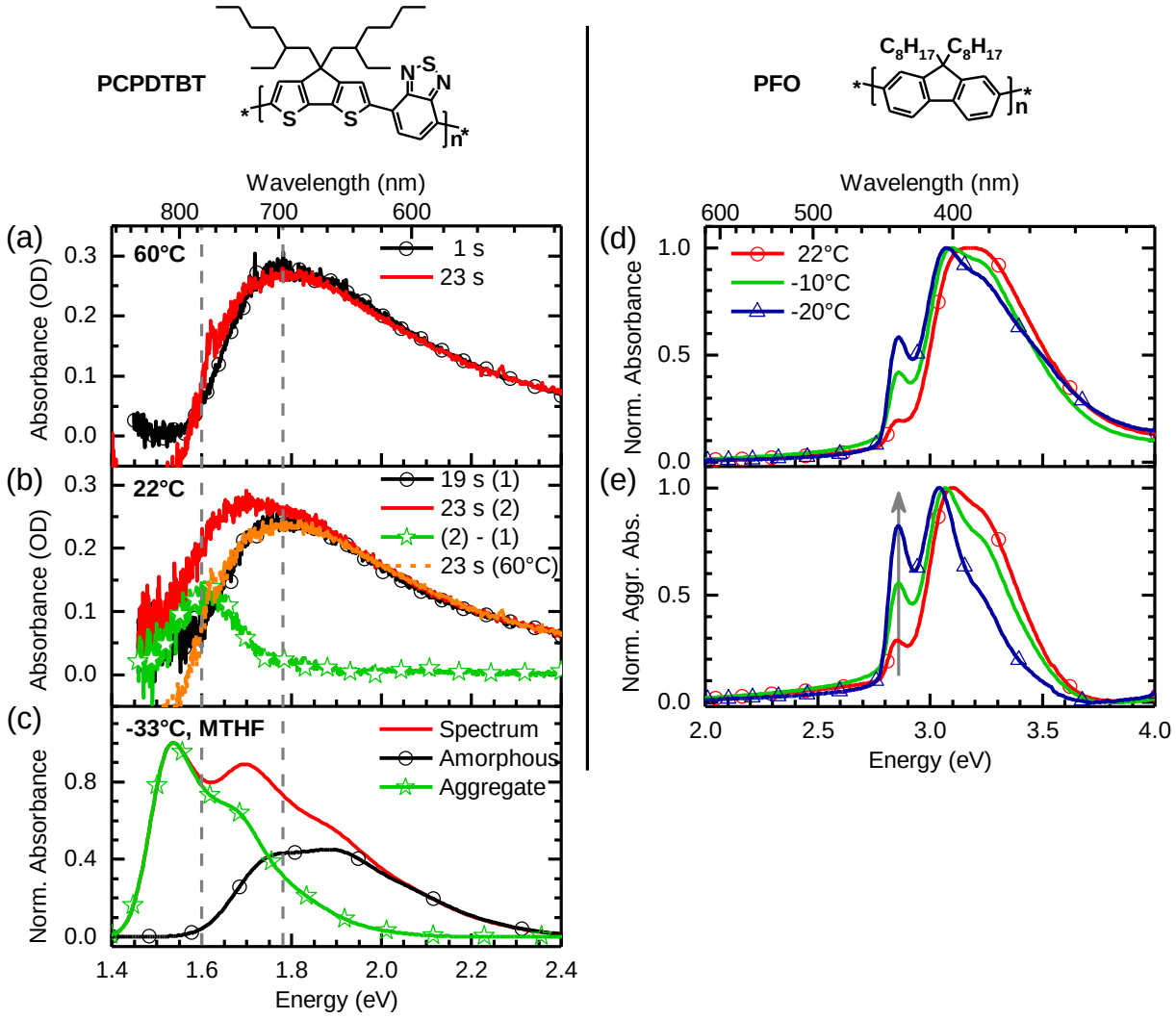

Figure 4: Absorption spectra of a PCPDTBT solution in CB ($c = 10\,\frac{g}{l}$) that was deposited onto substrates held at different temperatures, i.e. (a) 60°C and (b) 22°C, for different times during the spin-coating process. The chemical structure of PCPDTBT is shown on the top left. In (b), the green line with starts denotes the difference between the spectra at 19 s and 23 s. For comparison, the suitably normalized spectrum at 23 s on the 60°C substrate is also shown. (c) Normalized absorption spectrum of a PCPDTBT solution in MTHF at -33°C, i.e. below T_c ($c = 0.25\,\frac{g}{l}$), along with its separation into contributions attributed to aggregated polymer chains and nonaggregated polymer chains, taken from ref. [73]. (d) Absorption spectra of films spin-cast of a PFO solution in MTHF ($c = 3\,\frac{g}{l}$) at different temperatures, i.e. 22°C, -10°C and -20°C. The

chemical structure of PFO is shown on the top right (e) Aggregate absorption spectra in the β-phase of PFO films after spin-coating at different temperatures, extracted from the spectra in part d, and normalized to their maximum. The grey arrow is a guide to the eye.

References

1. Sirringhaus, H.; Brown, P. J.; Friend, R. H.; Nielsen, M. M.; Bechgaard, K.; Langeveld-Voss, B. M. W.; Spiering, A. J. H.; Janssen, R. A. J.; Meijer, E. W.; Herwig, P., et al. Two-Dimensional Charge Transport in Self-Organized, High-Mobility Conjugated Polymers. *Nature* **1999**, *401*, 685-688.

2. Yan, H.; Chen, Z. H.; Zheng, Y.; Newman, C.; Quinn, J. R.; Dotz, F.; Kastler, M.; Facchetti, A. A High-Mobility Electron-Transporting Polymer for Printed Transistors. *Nature* **2009**, *457*, 679-686.

3. Sirringhaus, H.; Kawase, T.; Friend, R. H.; Shimoda, T.; Inbasekaran, M.; Wu, W.; Woo, E. P. High-Resolution Inkjet Printing of All-Polymer Transistor Circuits. *Science* **2000**, *290*, 2123-2126.

4. He, Z. C.; Zhong, C. M.; Su, S. J.; Xu, M.; Wu, H. B.; Cao, Y. Enhanced Power-Conversion Efficiency in Polymer Solar Cells Using an Inverted Device Structure. *Nature Photonics* **2012**, *6*, 591-595.

5. Tremel, K.; Ludwigs, S. Morphology of P3HT in Thin Films in Relation to Optical and Electrical Properties. *Advanced Polymer Science* **2014**, *265*, 39-82.

6. Botiz, I.; Stingelin, N. Influence of Molecular Conformations and Microstructure on the Optoelectronic Properties of Conjugated Polymers. *Materials* **2014**, *7*, 2273-2300.

7. Treat, N. D.; Westacott, P.; Stingelin, N. The Power of Materials Science Tools for Gaining Insights into Organic Semiconductors. *Annual Review of Materials Research* **2015**, *45*, 459-490.

8. Silva, C.; Russell, D. M.; Dhoot, A. S.; Herz, L. M.; Daniel, C.; Greenham, N. C.; Arias, A. C.; Setayesh, S.; Mullen, K.; Friend, R. H. Exciton and Polaron Dynamics in a Step-Ladder

Polymeric Semiconductor: The Influence of Interchain Order. *Journal of Physics - Condensed Matter* **2002**, *14*, 9803-9824.

9. Khan, A. L. T.; Sreearunothai, P.; Herz, L. M.; Banach, M. J.; Köhler, A. Morphology-Dependent Energy Transfer Within Polyfluorene Thin Films. *Physical Review B* **2004**, *69*, 085201.

10. Ma, W. L.; Yang, C. Y.; Gong, X.; Lee, K.; Heeger, A. J. Thermally Stable, Efficient Polymer Solar Cells with Nanoscale Control of the Interpenetrating Network Morphology. *Advanced Functional Materials* **2005**, *15*, 1617-1622.

11. Hayer, A.; Khan, A. L. T.; Friend, R. H.; Köhler, A. Morphology Dependence of the Triplet Excited State Formation and Absorption in Polyfluorene. *Physical Review B* **2005**, *71*, 241302.

12. Li, G.; Zhu, R.; Yang, Y. Polymer Solar Cells. *Nature Photonics* **2012**, *6*, 153-161.

13. Liu, X. L.; Hüttner, S.; Rong, Z. X.; Sommer, M.; Friend, R. H. Solvent Additive Control of Morphology and Crystallization in Semiconducting Polymer Blends. *Advanced Materials* **2012**, *24*, 669-674.

14. Gruber, M.; Wagner, J.; Klein, K.; Hormann, U.; Opitz, A.; Stutzmann, M.; Brütting, W. Thermodynamic Efficiency Limit of Molecular Donor-Acceptor Solar Cells and its Application to Diindenoperylene/C60-Based Planar Heterojunction Devices. *Advanced Energy Materials* **2012**, *2*, 1100-1108.

15. Dang, M. T.; Hirsch, L.; Wantz, G.; Wuest, J. D. Controlling the Morphology and Performance of Bulk Heterojunctions in Solar Cells. Lessons Learned from the Benchmark Poly(3-hexylthiophene):[6,6]-Phenyl-C-61-butyric Acid Methyl Ester System. *Chemical Reviews* **2013**, *113*, 3734-3765.

16. Liu, Y. H.; Zhao, J. B.; Li, Z. K.; Mu, C.; Ma, W.; Hu, H. W.; Jiang, K.; Lin, H. R.; Ade, H.; Yan, H. Aggregation and Morphology Control Enables Multiple Cases of High-Efficiency Polymer Solar Cells. *Nature Communications* **2014**, *5*, 5293.

17. Scarongella, M.; Paraecattil, A. A.; Buchaca-Domingo, E.; Douglas, J. D.; Beaupre, S.; McCarthy-Ward, T.; Heeney, M.; Moser, J. E.; Leclerc, M.; Frechet, J. M. J., et al. The Influence of Microstructure on Charge Separation Dynamics in Organic Bulk Heterojunction Materials for Solar Cell Applications. *Journal of Materials Chemistry A* **2014**, *2*, 6218-6230.

18. Scarongella, M.; De Jonghe-Risse, J.; Buchaca-Domingo, E.; Causa, M.; Fei, Z. P.; Heeney, M.; Moser, J. E.; Stingelin, N.; Banerji, N. A Close Look at Charge Generation in Polymer:Fullerene Blends with Microstructure Control. *Journal of the American Chemical Society* **2015**, *137*, 2908-2918.

19. Dou, F.; Buchaca-Domingo, E.; Sakowicz, M.; Rezasoltani, E.; McCarthy-Ward, T.; Heeney, M.; Zhang, X. P.; Stingelin, N.; Silva, C. The Effect of Phase Morphology on the Nature of Long-Lived Charges in Semiconductor Polymer:Fullerene Systems. *Journal of Materials Chemistry C* **2015**, *3*, 3722-3729.

20. Kline, R. J.; McGehee, M. D.; Kadnikova, E. N.; Liu, J. S.; Frechet, J. M. J. Controlling the Field-Effect Mobility of Regioregular Polythiophene by Changing the Molecular Weight. *Advanced Materials* **2003**, *15*, 1519-1522.

21. Chang, J. F.; Sun, B. Q.; Breiby, D. W.; Nielsen, M. M.; Solling, T. I.; Giles, M.; McCulloch, I.; Sirringhaus, H. Enhanced Mobility of Poly(3-hexylthiophene) Transistors by Spin-Coating from High-Boiling-Point Solvents. *Chemistry of Materials* **2004**, *16*, 4772-4776.

22. Pingel, P.; Zen, A.; Abellon, R. D.; Grozema, F. C.; Siebbeles, L. D. A.; Neher, D. Temperature-Resolved Local and Macroscopic Charge Carrier Transport in Thin P3HT Layers. *Advanced Functional Materials* **2010**, *20*, 2286-2295.

23. An, T. K.; Kang, I.; Yun, H. J.; Cha, H.; Hwang, J.; Park, S.; Kim, J.; Kim, Y. J.; Chung, D. S.; Kwon, S. K., et al. Solvent Additive to Achieve Highly Ordered Nanostructural Semicrystalline DPP Copolymers: Toward a High Charge Carrier Mobility. *Advanced Materials* **2013**, *25*, 7003-7009.

24. Kim, N.-K.; Jang, S.-Y.; Pace, G.; Caironi, M.; Park, W.-T.; Khim, D.; Kim, J.; Kim, D.-Y.; Noh, Y.-Y. High-Performance Organic Field-Effect Transistors with Directionally Aligned Conjugated Polymer Film Deposited from Pre-Aggregated Solution. *Chemistry of Materials* **2015**, *27*, 8345-8353.

25. Herrmann, D.; Niesar, S.; Scharsich, C.; Köhler, A.; Stutzmann, M.; Riedle, E. Role of Structural Order and Excess Energy on Ultrafast Free Charge Generation in Hybrid Polythiophene/Si Photovoltaics Probed in Real Time by Near-Infrared Broadband Transient Absorption. *Journal of the American Chemical Society* **2011**, *133*, 18220-18233.

26. Roehling, J. D.; Arslan, I.; Moulé, A. J. Controlling Microstructure in Poly(3-hexylthiophene) Nanofibers. *Journal of Materials Chemistry* **2012**, *22*, 2498-2506.

27. Chang, L. L.; Lademann, H. W. A.; Bonekamp, J. B.; Meerholz, K.; Moulé, A. J. Effect of Trace Solvent on the Morphology of P3HT:PCBM Bulk Heterojunction Solar Cells. *Advanced Functional Materials* **2011**, *21*, 1779-1787.

28. Niles, E. T.; Roehling, J. D.; Yamagata, H.; Wise, A. J.; Spano, F. C.; Moulé, A. J.; Grey, J. K. J-Aggregate Behavior in Poly-3-hexylthiophene Nanofibers. *Journal of Physical Chemistry Letters* **2012**, *3*, 259-263.

29. Zhao, K.; Yu, X. H.; Li, R. P.; Amassian, A.; Han, Y. C. Solvent-Dependent Self-Assembly and Ordering in Slow-Drying Drop-Cast Conjugated Polymer Films. *Journal of Materials Chemistry C* **2015**, *3*, 9842-9848.

30. Zhao, K.; Khan, H. U.; Li, R. P.; Su, Y. S.; Amassian, A. Entanglement of Conjugated Polymer Chains Influences Molecular Self-Assembly and Carrier Transport. *Advanced Functional Materials* **2013**, *23*, 6024-6035.

31. Hu, H. L.; Zhao, K.; Fernandes, N.; Boufflet, P.; Bannock, J. H.; Yu, L. Y.; de Mello, J. C.; Stingelin, N.; Heeney, M.; Giannelise, E. P., et al. Entanglements in Marginal Solutions: a Means of Tuning Pre-Aggregation of Conjugated Polymers with Positive Implications for Charge Transport. *Journal of Materials Chemistry C* **2015**, *3*, 7394-7404.

32. Kleinhenz, N.; Persson, N.; Xue, Z. Z.; Chu, P. H.; Wang, G.; Yuan, Z. B.; McBride, M. A.; Choi, D.; Grover, M. A.; Reichmanis, E. Ordering of Poly(3-hexylthiophene) in Solutions and Films: Effects of Fiber Length and Grain Boundaries on Anisotropy and Mobility. *Chemistry of Materials* **2016**, *28*, 3905-3913.

33. Choi, D.; Chang, M.; Reichmanis, E. Controlled Assembly of Poly(3-hexylthiophene): Managing the Disorder to Order Transition on the Nano- Through Meso-Scales. *Advanced Functional Materials* **2015**, *25*, 920-927.

34. Aiyar, A. R.; Hong, J. I.; Nambiar, R.; Collard, D. M.; Reichmanis, E. Tunable Crystallinity in Regioregular Poly(3-Hexylthiophene) Thin Films and Its Impact on Field Effect Mobility. *Advanced Functional Materials* **2011**, *21*, 2652-2659.

35. Gao, Y. Q.; Martin, T. P.; Niles, E. T.; Wise, A. J.; Thomas, A. K.; Grey, J. K. Understanding Morphology-Dependent Polymer Aggregation Properties and Photocurrent Generation in Polythiophene/Fullerene Solar Cells of Variable Compositions. *Journal of Physical Chemistry C* **2010**, *114*, 15121-15128.

36. Scharsich, C.; Lohwasser, R. H.; Sommer, M.; Asawapirom, U.; Scherf, U.; Thelakkat, M.; Neher, D.; Köhler, A. Control of Aggregate Formation in Poly(3-hexylthiophene) by Solvent, Molecular Weight, and Synthetic Method. *Journal of Polymer Science Part B: Polymer Physics* **2012**, *50*, 442-453.

37. Na, J. Y.; Kang, B.; Sin, D. H.; Cho, K.; Park, Y. D. Understanding Solidification of Polythiophene Thin Films during Spin-Coating: Effects of Spin-Coating Time and Processing Additives. *Scientific Reports* **2015**, *5*, 13288.

38. Peet, J.; Cho, N. S.; Lee, S. K.; Bazan, G. C. Transition from Solution to the Solid State in Polymer Solar Cells Cast from Mixed Solvents. *Macromolecules* **2008**, *41*, 8655-8659.

39. Lee, J. K.; Ma, W. L.; Brabec, C. J.; Yuen, J.; Moon, J. S.; Kim, J. Y.; Lee, K.; Bazan, G. C.; Heeger, A. J. Processing additives for improved efficiency from bulk heterojunction solar cells. *Journal of the American Chemical Society* **2008**, *130*, 3619-3623.

40. Peet, J.; Kim, J. Y.; Coates, N. E.; Ma, W. L.; Moses, D.; Heeger, A. J.; Bazan, G. C. Efficiency Enhancement in Low-Bandgap Polymer Solar Cells by Processing with Alkane Dithiols. *Nature Materials* **2007**, *6*, 497-500.

41. Peet, J.; Brocker, E.; Xu, Y.; Bazan, G. C. Controlled β-Phase Formation in Poly(9,9-di-n-octylfluorene) by Processing with Alkyl Additives. *Advanced Materials* **2008**, *20*, 1882-1885.

42. Arca, F.; Loch, M.; Lugli, P. Enhancing Efficiency of Organic Bulkheterojunction Solar Cells by Using 1,8-Diiodooctane as Processing Additive. *Ieee Journal of Photovoltaics* **2014**, *4*, 1560-1565.

43. Clarke, T. M.; Peet, J.; Lungenschmied, C.; Drolet, N.; Lu, X. H.; Ocko, B. M.; Mozer, A. J.; Loi, M. A. The Role of Emissive Charge Transfer States in Two Polymer-Fullerene Organic Photovoltaic Blends: Tuning Charge Photogeneration Through the Use of Processing Additives. *Journal of Materials Chemistry A* **2014**, *2*, 12583-12593.

44. Reichenberger, M.; Baderschneider, S.; Kroh, D.; Grauf, S.; Köhler, J.; Hildner, R.; Köhler, A. Watching Paint Dry: The Impact of Diiodooctane on the Kinetics of Aggregate Formation in Thin Films of Poly(3-hexylthiophene). *Macromolecules* **2016**, *49*, 6420-6430.

45. Panzer, F.; Bässler, H.; Köhler, A. Temperature Induced Order-Disorder Transition in Solutions of Conjugated Polymers Probed by Optical Spectroscopy. *Journal of Physical Chemistry Letters* **2017**, *8*, 114-125.

46. Perevedentsev, A.; Stavrinou, P. N.; Smith, P.; Bradley, D. D. C. Solution-Crystallization and Related Phenomena in 9,9-Dialkyl-Fluorene Polymers. II. Influence of Side-Chain Structure. *Journal of Polymer Science Part B: Polymer Physics* **2015**, *53*, 1492-1506.

47. Perevedentsev, A.; Stavrinou, P. N.; Bradley, D. D. C.; Smith, P. Solution-Crystallization and Related Phenomena in 9,9-Dialkyl-Fluorene Polymers. I. Crystalline Polymer-Solvent Compound Formation for Poly(9,9-dioctylfluorene). *Journal of Polymer Science Part B: Polymer Physics* **2015**, *53*, 1481-1491.

48. Yang, Y.; Mielczarek, K.; Zakhidov, A.; Hu, W. Efficient Low Bandgap Polymer Solar Cell with Ordered Heterojunction Defined by Nanoimprint Lithography. *Acs Applied Materials & Interfaces* **2014**, *6*, 19282-19287.

49. Kesters, J.; Verstappen, P.; Raymakers, J.; Vanormelingen, W.; Drijkoningen, J.; D'Haen, J.; Manca, J.; Lutsen, L.; Vanderzande, D.; Maes, W. Enhanced Organic Solar Cell Stability by Polymer (PCPDTBT) Side Chain Functionalization. *Chemistry of Materials* **2015**, *27*, 1332-1341.

50. Albrecht, S.; Janietz, S.; Schindler, W.; Frisch, J.; Kurpiers, J.; Kniepert, J.; Inal, S.; Pingel, P.; Fostiropoulos, K.; Koch, N., et al. Fluorinated Copolymer PCPDTBT with Enhanced Open-Circuit Voltage and Reduced Recombination for Highly Efficient Polymer Solar Cells. *Journal of the American Chemical Society* **2012**, *134*, 14932-14944.

51. Fischer, F. S. U.; Trefz, D.; Back, J.; Kayunkid, N.; Tornow, B.; Albrecht, S.; Yager, K. G.; Singh, G.; Karim, A.; Neher, D., et al. Highly Crystalline Films of PCPDTBT with Branched Side Chains by Solvent Vapor Crystallization: Influence on Opto-Electronic Properties. *Advanced Materials* **2015**, *27*, 1223-1228.

52. Albrecht, S.; Schafer, S.; Lange, I.; Yilmaz, S.; Dumsch, I.; Allard, S.; Scherf, U.; Hertwig, A.; Neher, D. Light Management in PCPDTBT:$PC_{70}BM$ solar cells: A Comparison of Standard and Inverted Device Structures. *Organic Electronics* **2012**, *13*, 615-622.

53. Perevedentsev, A.; Chander, N.; Kim, J. S.; Bradley, D. D. C. Spectroscopic Properties of Poly(9,9-dioctylfluorene) Thin Films Possessing Varied Fractions of b-Phase Chain Segments: Enhanced Photoluminescence Efficiency via Conformation Structuring. *Journal of Polymer Science Part B: Polymer Physics* **2016**, *54*, 1995-2006.

54. Kleinschmidt, A. T.; Root, S. E.; Lipomi, D. J. Poly(3-hexylthiophene) (P3HT): Fruit Fly or Outlier in Organic Solar Cell Research? *Journal of Materials Chemistry A* **2017**, *5*, 11396-11400.

55. Heffner, G. W.; Pearson, D. S. Molecular Characterization of Poly(3-Hexylthiophene). *Macromolecules* **1991**, *24*, 6295-6299.

56. Grauf, S. *Einfluss der Prozessiertemperatur auf die Dünnschichtmorphologie konjugierter Polymere*. Bachelor's Thesis **2015**, University of Bayreuth.

57. Abdelsamie, M.; Zhao, K.; Niazi, M. R.; Chou, K. W.; Amassian, A. In Situ UV-Visible Absorption During Spin-Coating of Organic Semiconductors: A New Probe for Organic Electronics and Photovoltaics. *Journal of Materials Chemistry C* **2014**, *2*, 3373-3381.

58. Jiang, Z. GIXSGUI: A MATLAB Toolbox for Grazing-Incidence X-Ray Scattering Data Visualization and Reduction, and Indexing of Buried Three-Dimensional Periodic Nanostructured Films. *Journal of Applied Crystallography* **2015**, *48*, 917-926.

59. Panzer, F.; Bässler, H.; Lohwasser, R.; Thelakkat, M.; Köhler, A. The Impact of Polydispersity and Molecular Weight on the Order-Disorder Transition in Poly(3-hexylthiophene). *Journal of Physical Chemistry Letters* **2014**, *5*, 2742-2747.

60. Berson, S.; De Bettignies, R.; Bailly, S.; Guillerez, S. Poly (3-hexylthiophene) Fibers for Photovoltaic Applications. *Advanced Functional Materials* **2007**, *17*, 1377-1384.

61. Clark, J.; Chang, J. F.; Spano, F. C.; Friend, R. H.; Silva, C. Determining Exciton Bandwidth and Film Microstructure in Polythiophene Films Using Linear Absorption Spectroscopy. *Applied Physics Letters* **2009**, *94*, 163306.

62. Yonkoski, R. K.; Soane, D. S. Model for Spin Coating in Microelectronic Applications. *Journal of Applied Physics* **1992**, *72*, 725-740.

63. Askeland, D. R.; Fulay, P. P.; Wright, W. J. *The Science And Engineering of Materials*. Wadsworth Publishing Co Inc.: Belmont, **2010**.

64. Srirachat, W.; Wannachod, T.; Pancharoen, U.; Kheawhom, S. Effect of Polarity and Temperature on the Binary Interaction Between D2EHPA Extractant and Organic Solvents (Kerosene, n-Heptane, Chlorobenzene and 1-Octanol): Experimental and Thermodynamics. *Fluid Phase Equilibria* **2017**, *434*, 117-129.

65. Köhler, A.; Hoffmann, S. T.; Bässler, H. An Order-Disorder Transition in the Conjugated Polymer MEH-PPV. *Journal of the American Chemical Society* **2012**, *134*, 11594-11601.

66. De Leener, C.; Hennebicq, E.; Sancho-Garcia, J. C.; Beljonne, D. Modeling the Dynamics of Chromophores in Conjugated Polymers: The Case of Poly (2-methoxy-5-(2 '-ethylhexyl)oxy 1,4-phenylene vinylene) (MEH-PPV). *Journal of Physical Chemistry B* **2009**, *113*, 1311-1322.

67. Hellmann, C.; Treat, N. D.; Scaccabarozzi, A. D.; Hollis, J. R.; Fleischli, F. D.; Bannock, J. H.; de Mello, J.; Michels, J. J.; Kim, J. S.; Stingelin, N. Solution Processing of Polymer Semiconductor:Insulator Blends - Tailored Optical Properties Through Liquid-Liquid Phase Separation Control. *Journal of Polymer Science Part B - Polymer Physics* **2015**, *53*, 304-310.

68. Spano, F. C. Modeling Disorder in Polymer Aggregates: The Optical Spectroscopy of Regioregular Poly(3-hexylthiophene) Thin Films. *Journal of Chemical Physics* **2005**, *122*, 234701.

69. Spano, F. C. Absorption in Regio-Regular Poly(3-hexyl)thiophene Thin Films: Fermi Resonances, Interband Coupling and Disorder. *Chemical Physics* **2006**, *325*, 22-35.

70. Spano, F. C. The Spectral Signatures of Frenkel Polarons in H- and J-Aggregates. *Accounts of Chemical Research* **2010**, *43*, 429-439.

71. Panzer, F.; Sommer, M.; Bassler, H.; Thelakkat, M.; Kohler, A. Spectroscopic Signature of Two Distinct H-Aggregate Species in Poly(3-hexylthiophene). *Macromolecules* **2015**, *48*, 1543-1553.

72. Reichenberger, M.; Love, J. A.; Rudnick, A.; Bagnich, S.; Panzer, F.; Stradomska, A.; Bazan, G. C.; Nguyen, T. Q.; Köhler, A. The Effect of Intermolecular Interaction on Excited States in p-DTS(FBTTH$_2$)$_2$. *Journal of Chemical Physics* **2016**, *144*, 074904.

73. Scharsich, C.; Fischer, F. S. U.; Wilma, K.; Hildner, R.; Ludwigs, S.; Köhler, A. Revealing Structure Formation in PCPDTBT by Optical Spectroscopy. *Journal of Polymer Science Part B: Polymer Physics* **2015**, *53*, 1416-1430.

74. Spano, F. C.; Silva, C. H- and J-Aggregate Behavior in Polymeric Semiconductors. *Annual Review of Physical Chemistry* **2014**, *65*, 477-500.

75. Kolinski, A.; Skolnick, J.; Yaris, R. The Collapse Transition of Semiflexible Polymers - a Monte-Carlo Simulation of a Model System. *Journal of Chemical Physics* **1986**, *85*, 3585-3597.

76. Sanchez, I. C. Phase-Transition Behavior of the Isolated Polymer-Chain. *Macromolecules* **1979**, *12*, 980-988.